2018 15th International Conference on
Control, Automation, Robotics and Vision (ICARCV)
Singapore, November 18-21, 2018

Vision Based Automatic Landing with Runway Identification and Tracking

Amit Kumar Tripathi[1], Vijay V Patel[2], Radhakant Padhi[3]

***Abstract*— Vision based autolanding of a fixed wing unmanned aerial vehicle (UAV) is presented in this paper. The UAV initially searches for a nearby unknown road or runway from the terrain image frames captured by onboard stereovision camera. The captured unknown road or runway are evaluated to be a possible candidate for autolanding of a UAV. Six degree of freedom $(6DOF)$ simulink model of a UAV with landing and navigation autopilot is integrated with flightgear flight simulation software. Flightgear FG camera is used to capture image frames of the nearyby terrain while UAV is in auto navigation mode and performing a level flight with various heading angles to look out for all possible terrain scenario. Image processing techniques are applied on the captured video to identify a smooth and straight road or runway for landing and calculates the relative distance and orientation of the runway or road with respect to UAV's own location. Image processing techniques such as hough transform and random Sample consensus (RANSAC) are used to detect the road strip lines. Once the desired touchdown point on the road is computed as well as road heading is also computed, UAV begins the autolanding maneuver. The image processing techniques are used to identify the candidate road or runway. The heading of the runway and cross track of the runway is computed and autopilot is designed to bring the aircraft at desired touch down point on the road or runway.**

I. INTRODUCTION

The vision based autonomous landing plays a very important role for small UAVs. The UAV's are lightweight and carry limited fuel. UAVs are also not augmented with expensive sensors. UAVs are generally used for surveillance and reconnaissance purposes apart from many other important applications. UAVs generally cruise at low altitude and carry inexpensive stereovision sensors which are fairly good to the extent of capturing aerial images with good clarity. Small UAVs fly or cruise at low speeds so image frame uncertainty with respect to UAV position can also be lower compared to the one which is flying with higher speeds.

Runway or road identification for autolanding of the UAV is carried out by keeping all the performance criteria like availability of straight road to facilitate the autolanding distance of the UAV, no significant obstacles or patches in the straight line portion of the road, availability of landing distance, no curvatures etc. Image processing techniques like image segamentation, morphological techniques, corner detection techniques, median and gaussian filters are used to process the captured terrain image frames.

[1]Amit K. Tripathi is Scientist with Aeronautical Development Agency, Bangalore, India amitktripathi@gmail.com

[2]Vijay V Patel is Scientist with Aeronautical Development Agency, Bangalore, India vvp2069@yahoo.com

[2]Radhakant Padhi is Faculty of Aerospace Engineering, Indian Institute of Science, Bangalore, India padhi@iisc.ac.in

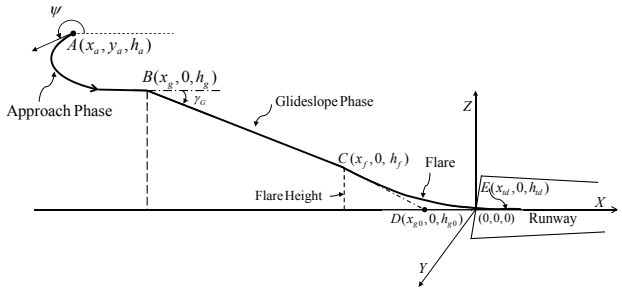

Fig. 1. Auto landing Phase of a Unmanned Aerial Vehicle

Vision aided navigation requires no on ground infrastructure. An approach towards estimating candidate road or runway position is presented here. An onboard stereovision camera senses the terrain and after completing image frames processing estimates runway position, runway orientation as well as the cross track error. This method utilizes the approximate information about the aircraft or onboard camera position and orientation to obtain a two-dimensional (2D) projection of the runway on the image plane. Stereo vision camera sensors based runway detection algorithm has been proposed in literature. Runway detection in an image sequence has been proposed in [11]

The Autonomous landing comprise of mainly three phases [1] such as alignment and approach phase, where UAV aligns with the runway by correcting the heading. Next is glideslope phase, where the UAV follows a fixed ramp path with constant flight path angle until it reaches a flare height. During the glideslope phase UAV descends with a higher sink rate. Once the flare height is achieved the UAV follows a exponential trajectory until the touchdown point. During the flare trajectory the UAV is closer to ground, sink rate is reduced and the UAV descends under stricter controller requirements than the glideslope phase. Flare is an important phase of UAV and the altitude control should be very efficient as well as ground effects [7] are also dominant in this phase. The different phases of autolanding is shown in Fig. 1.

In this paper NDI based autopilot is used to perform autolanding operation of UAVs.

The prime objective of this paper is rapid detection of the runway in an image sequence captured from a landing aircraft or UAV. In case of manned aircraft, Pilot aiding during low-altitude flight has been an important research topic in the field of navigation. During the critical section of landing maneuvers, a vision system which can continuously detect the runway is very useful to both enhance the landing

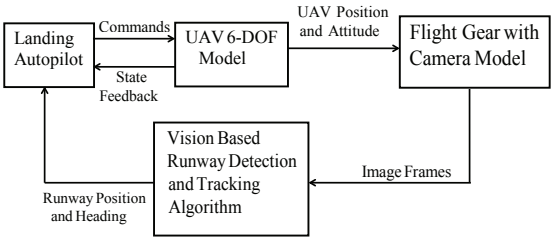

Fig. 2. Vision based Auto landing System

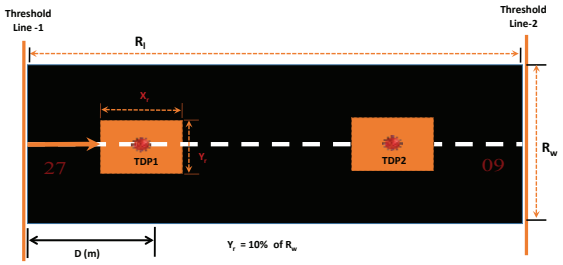

Fig. 3. Desired Touchdown Point

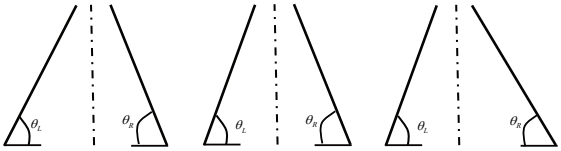

Fig. 4. Runway Edge Slopes under different View Point

safety and reduce the pilot's workload. Such system requires fast and reliable recognition strategies in order to meet the real-time flight control demand.

II. Vision Based Autolanding Problem Formulation

Closed loop system with landing autopilot and image processing feedback is shown in Fig. 2. UAV onboard camera looks ahead and captures real time terrain image frames. Onboard Image processing system processes the real time video and computes the runway position with respect to the UAV. The landing autopilot uses the runway position information and guides the UAV land on the intended runway with acceptable error margins.

III. Runway Identification and Tracking

This section describes various image processing techniques used in runway identification.

A. Information Required for Landing on an Airfield

Image processing is used to identify the suitable terrain for autolanding of aircraft or UAV. It requires a smooth surface with a width typically $50 - 60$ meters and length which can suffice the landing distance of UAV. Therefore latitude, longitude altitude of the Threshold Points on the airfield are required. Azimuth and elevation angles, slant distance with respect to threshold points to UAV are required to be known. This can be used to compute cross track error and heading of the runway.

B. Desired Touchdown Point on Airfield

Desired Touchdown Point on Airfield is shown in Fig. 3. Touchdown points(TDP1 and TDP2) are representative points on the airfield subject to their direction of approach to the airfield. The numbers 09 and 27 marked across each threshold indicate the heading angle of 90 degree and 270 degree respectively.

1) Runway Model: Runway model edges lines are shown in Fig. 4. The slopes of runway lines are θ_L and θ_R respectively. If UAV is aligned with runway central line, both runway lines slope angles will be equal. If UAV is not aligned with runway central line, runway lines slope angles will not be equal.

- If $\theta_R > \theta_L$, UAV on right side of the runway and should fly towards left to align with runway central line
- If $\theta_L = \theta_R$, UAV on runway central line and should fly towards runway central line
- If $\theta_L > \theta_R$, UAV on left side of the runway and should fly towards right to align with runway central line

Runway central line making an angle θ_c as shown in Fig. 5, then using algebraic calculations following equations can be obtained.

$$\tan\theta_c = \frac{2\sin\theta_L \sin\theta_R}{\sin(\theta_L - \theta_R)} \tag{1}$$

Runway width in pixel, angle or slope of the edge lines and focal length of the camera can be obtained from onboard camera captured image frames through image processing.

The image frame captured through flightgear camera during landing of a UAV as shown in Fig. 6. Runway line slope as viewed from UAV is 83^0 for left runway line and 68^0 for right runway line using hough line detection. Runway central line angle in image plane is computed from Eq. (1) as 81.995^0. However knowing runway heading is 90^0. It can be inferred that a shift of 8^0 is required to align with runway.

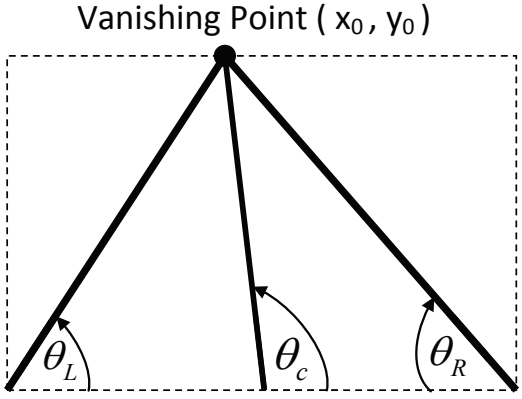

Fig. 5. Runway Central line Slope Computation

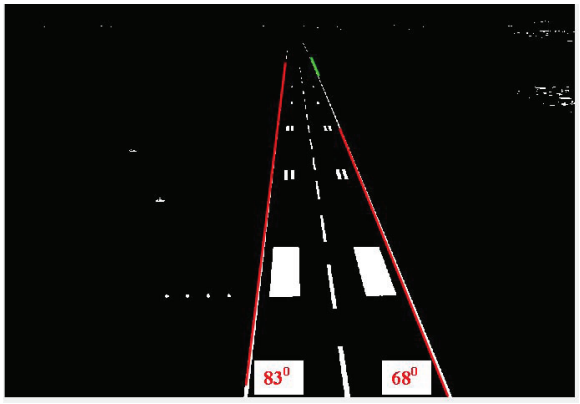

Fig. 6. Heading offset Error Computation from Hough line slopes

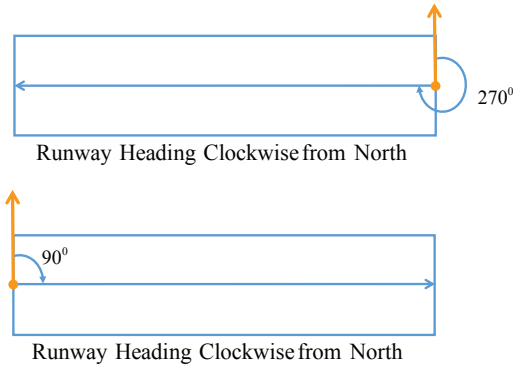

Fig. 7. Runway Heading Clockwise from North

2) Runway Heading Angle: The heading of the airfield is always measured clockwise from north. In the Fig. 7 heading directions from both approach sides are shown.

C. Heading Angle or Bearing Angle

Bearing or heading angle of a point with respect to another point is described here. Bearing would be measured from North direction i.e 0^0 bearing means North, 90^0 bearing is East, 180^0 bearing is measured to be South, and 270^0 to be West. However, if bearing is denoted with positive or negative sign initials whose values lies between 0^0 to 180^0, then negative sign is denoted for South and West sides. If latitude, longitude information of two different points (A and B) are given, bearing from point A to B, can be calculated as follows.

$$\beta = \text{atan2}(X, Y) \tag{2}$$

where, X and Y are two quantities and can be calculated as follows

$$X = \cos\theta_b \sin\Delta L \tag{3}$$
$$Y = \cos\theta_a \sin\theta_b - \sin\theta_a \cos\theta_b \cos\Delta L \tag{4}$$

where, L is longitude, $\Delta L = L_b - L_a$, θ is latitude, β is bearing or heading angle.

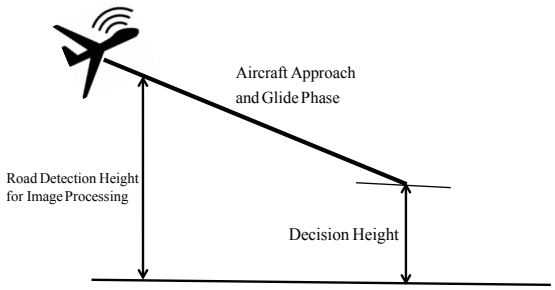

Fig. 8. Vision based Auto landing System

D. Decision Height

The Decision Altitude (DA) or Decision Height (DH) as shown in the Fig. 8 is a specified altitude or height in the Precision Approach or approach with vertical guidance at which a Missed Approach must be initiated if the required visual reference to continue the approach has not been established.

IV. Image Processing Techniques

This section describes various image processing techniques used in performing vision based autolanding of UAV

A. Image Segmentation

Image threshold and filtering is a image processing technique to obtain the region of interest [15]. In case of flightgear runway image frames a threshold of $180-190$ has been applied on grey image to obtain the runway edge markers. The other unwanted patterns and unwanted patches in the segmented image can be eliminated using morphological techniques.

B. Morphological Dilation and Erosion

Morphology is a broad set of image processing operations that process images based on shapes. Morphological operations apply a structuring element to an input image, creating an output image of the same size. By choosing the size and shape of the neighborhood, you can construct a morphological operation that is sensitive to specific shapes in the input image. Dilation and erosion are defined as follows

1) Dilation: The value of the output pixel is the maximum value of all the pixels in the input pixel's neighborhood. In a binary image, if any of the pixels is set to the value 1, the output pixel is set to 1.

2) Erosion: The value of the output pixel is the minimum value of all the pixels in the input pixel's neighborhood. In a binary image, if any of the pixels is set to 0, the output pixel is set to 0.

C. Edge detection

Edge detectors are used to find the areas where there is sharp changes in the gradients [16]. Here in this paper our objective is to identify runway edge markers. Edge detection technique used in the current work is canny edge detector.

D. Hough Transform

Hough Transform is used to find lines in an image. The block outputs the Hough space matrix and, optionally, the rho-axis and theta-axis vectors. Peak values in the matrix represent potential lines in the input image. Generally, the Hough Transform block precedes the Hough Lines block which uses the output of this block to find lines in an image. You can instead use a custom algorithm to locate peaks in the Hough space matrix in order to identify potential lines.

E. Random Sample Consensus

Random Sample Consensus(RANSAC) is used here as points to line converter [14]. The steps of RANSAC algorithm are described as follows

Randomly select a sample of s data points from data set S and instantiate the model from this subset. $s = 2$. Determine the set of data points Si which are within a distance threshold T of the model. The set Si is the consensus set of samples and defines the inliers of S. If the subset of Si is greater than some threshold T, re estimate the model using all the points in Si and terminate. If the size of Si is less than T, select a new subset and repeat the above. After N trials the largest consensus set Si is selected, and the model is re-estimated using all the points in the subset Si.

F. Structure from Motion

Structure from motion is a very powerful technique to generate $3D$ images. $3D$ images are generated based on sequence of multiple images captured by camera and matching the important feature points. Five sequence of Images are used in this section to generate the $3D$ reconstruction. The objective of SFM is to detect any obstacle on the road.

V. Runway detector Logic

A. Slant Distance Computation

The slant distance L between runway center line threshold point and camera focal point can be computed as shown in the Fig. 9. Physical runway width across threshold line is denoted by W_R, image frame pixel width is denoted by W_P, focal length of flightgear camera is denoted by f, azimuth and elevation angles of slant distance with respect to runway coordinates is represented by ψ_h and θ_h respectively.

Based on the triangle relationship as shown in the Fig. 9, the following equation can be derived.

$$\frac{W_R}{L} = \frac{W_p}{f} \tag{5}$$

In general, road or runway are constructed with standard width. Therefore, runway or road actual width W_p is considered to be around (50-60) m. Slant range L can be computed from Eq.(5). Image processing can be used to compute ψ_h and θ_h angles by processing runway central line threshold point. Cross track error (CTE), Horizontal range (X) and altitude (H) can be computed as follows

$$CTE = L\cos\theta_h \sin\psi_h \tag{6}$$

$$X = L\cos\theta_h \cos\psi_h \tag{7}$$

$$H = L\sin\theta_h \tag{8}$$

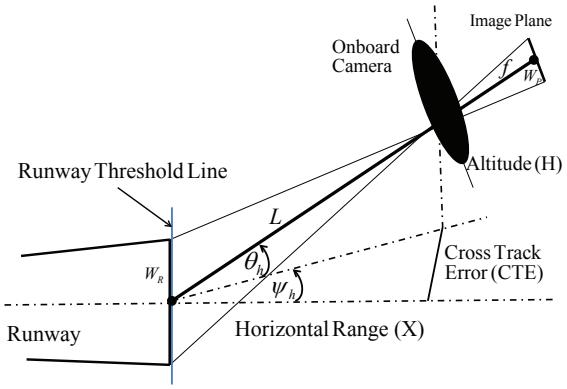

Fig. 9. Slant Distance Computation

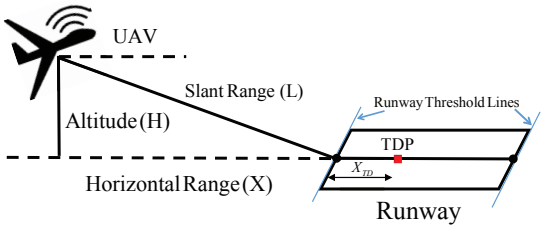

Fig. 10. TDP Forward Distance Computation

B. TDP Distance Computation

UAV current location to runway touch down point forward distance computation is shown in the Fig. 10. Distance across runway central line up to runway touch down point (TDP) can be computed as follows

$$\text{Total Forward Distance} = X + X_{TD} \tag{9}$$

C. Flight Gear Camera Focal Length Computation

Flight gear Camera Field of View (FOV) is set as 60^0 in present work. Focal length f of the flight gear camera can be calculated as follows as shown in the Fig. 11.

$$f = \frac{\left(\frac{\mathrm{w}}{2}\right)}{\tan\left(\frac{FOV}{2}\frac{pi}{180}\right)} \tag{10}$$

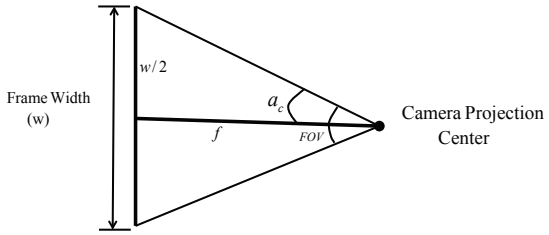

Fig. 11. Flightgear Camera Focal Length Computation

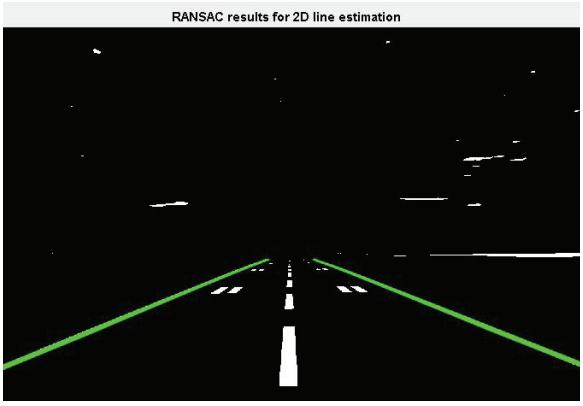

Fig. 12. Runway Edge lines detection with RANSAC algorithm

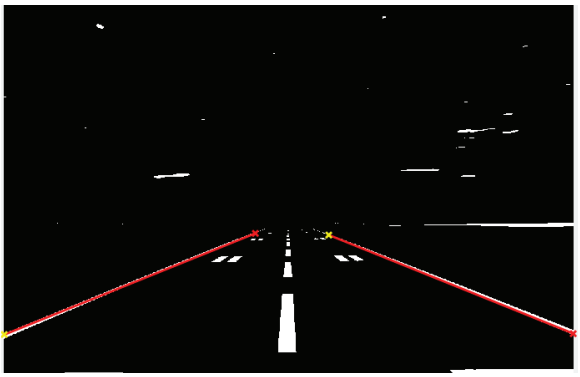

Fig. 13. Runway Edge lines detection with Hough algorithm

D. Hough-RANSAC Comparision

The Fig. 12 and Fig. 13 show the performance of RANSAC algorithm and Hough algorithm for runway line estimation. It can be seen that RANSAC algorithm estimates runway line better than Hough. Where ever actual white markers are weak, hough lines fail to detect the line but RANSAC detects that with a resonable accuracy.

VI. Path Planning and Guidance Design for Automatic Landing

The Auto landing maneuver has three important phases 1. Approach phase 2. glideslope phase and 3. flare phase. All the three phases are described in the following subsections

1) Approach Phase: Approach phase is usually course and track alignment phase where UAV aligns its track and course along with the runway. Once UAV aligns with the runway, cross track error becomes zero and its track angle is same as runway track angle.

2) Glideslope Descent Phase: In the glideslope descent, UAV follows a constant flight path angle γ trajectory. The typical reference γ_R is in the range $2.5^\circ - 3.5^\circ$ deg. The deviation d from fixed γ line is computed as follows

$$d = L \sin \delta \tag{11}$$

$$d = L \sin(\gamma - \gamma_R) \tag{12}$$

where L is the slant range of the UAV [5]

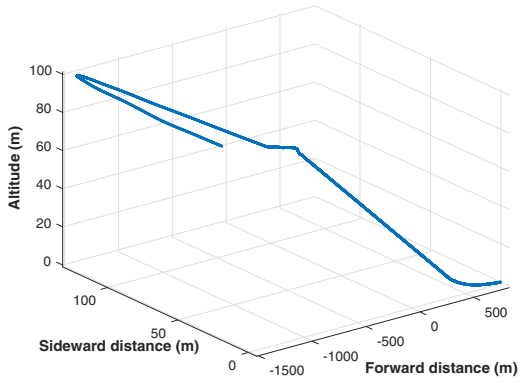

Fig. 14. Autolanding trajectory of an Aircraft

3) Flare Phase: Flare trajectory can be computed as follows

$$h(t) = h_f \exp^{-t/\tau} - 1 \tag{13}$$

where h_f is flare height. The commanded height h_c can be given as

$$h_c = h_f \exp^{-t/\tau} - 1 \tag{14}$$

$$\dot{h}_c = -h_f \frac{\exp^{-t/\tau}}{\tau} \tag{15}$$

$$\dot{h}_c = -\frac{h_c + 1}{\tau} \tag{16}$$

$$\ddot{h}_c = \frac{h_c + 1}{\tau^2} \tag{17}$$

Sink rate $\dot{h}$ can also be computed from velocity and flight path angle as follows

$$\dot{h} = V \sin \gamma \tag{18}$$

A. Nonlinear UAV State Dynamics

Assuming airplane to be a rigid body and earth to be flat the complete set of six-DOF equations are provided in [2], [8]. Autonomous landing problem of All Electric-2 (AE-2) aircraft is considered. Nonlinear six degrees of freedom (6DOF) model is taken from data available in [3].

VII. Simulation Results

The aircraft modeling and simulation is carried out as per [9] and [10]. Vision based autolanding trajectory is shown in the Fig. 14. UAV initially searches at $100m$ altitude for a possible runway and once runway identified, it begins autolanding.

Vision based autolanding longitudinal states are shown in the Fig. 15. Based on touch down point, reverse autolanding trajectory is computed and landing is initiated accordingly as the lateral offsets are zero.

Vision based autolanding lateral states are shown in the Fig. 16. Aircraft desired heading and track is obtained from image processing of the video data containing the runway.

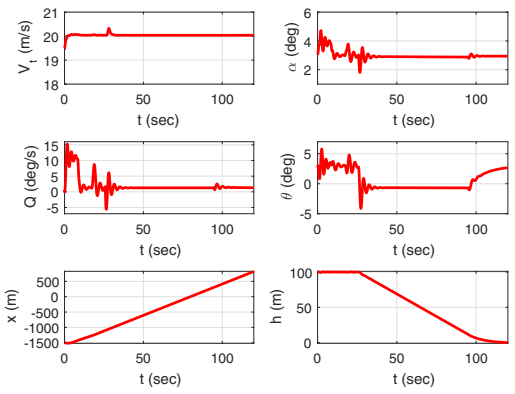

Fig. 15. Autolanding longitudinal states of an Aircraft

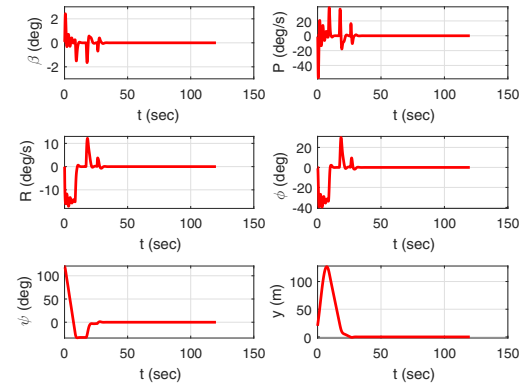

Fig. 16. Autolanding lateral-directional states of an Aircraft

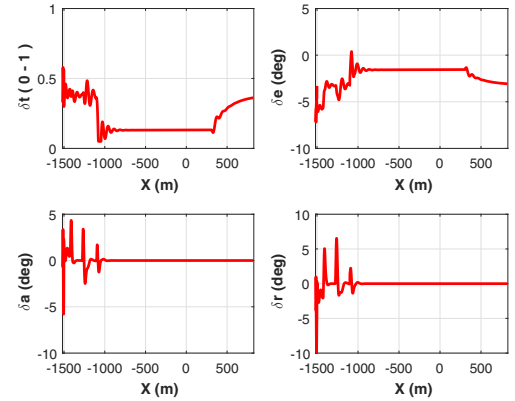

Fig. 17. Autolanding control command of an Aircraft

Vision based autolanding control commands for thrust δt, elevator deflection δ_e , aileron deflection δ_a and rudder deflection δ_r are shown in the Fig. 17.

Simulation results show that stereovision guided controller performs autolanding at the intended runway within acceptable performance bounds.

VIII. CONCLUSIONS

The autonomous landing problem for aircraft with six degree of freedom (6DOF) has been attempted using vision based runway identification and tracking. Vision based sensors are used to compute slant distance, azimuth and elevation angles of the touchdown point with respect to UAVs own position. Thus, absolute position of the runway is computed. Image processing techniques like image segmentation, edge detection, morphological filtering, Hough transform and RANSAC algorithms were used. Simulink-flightgear based simulation environment is used to carry out the auto landing simulations. Future task will include vision based autolanding with aerodynamic parameter uncertainities, ground effect and wind shear uncertainties using kalman filter estimation.

REFERENCES

[1] Prasad, B. and Pradeep S.,Automatic Landing System Design using Feedback Linearization Method, AIAA Conference and Exhibit, Rohnert Park, California, 7-10 May, 2007.

[2] B. Stevens and F. Lewis, "Aircraft Control and Simulation 2^{nd} Edition", *J. Wiley & Sons*, 2003.

[3] Surendra nath, V., Govindaraju, S. P., Bhat, M. S., and Rao, C. S. N., Configuration Development of All Electric Mini Airplane, ADE/DRDO Project, Project Ref. No: ADEO/MAE/VSU/001, Department of Aerospace Engg., IISc, Bangalore.

[4] Wang, R. , Zhou, Z. and Shen, Y., Flying Wing UAV Landing Control and Simulation Based on Mixed $H2/H\infty$, Proceedings of IEEE International Conference on Mechatronics and Automation, 1523–1528, Harbin, China, 2007

[5] Ghassan M. Amteh, Wahba I. Al-Taq and Zeaid Hasan, A Nonlinear Automatic Landing Control System for a UAV, Proceedings of the ASME 2011 International Mechanical Engineering Congress and Exposition, November 11–17, 2011, Denver, Colorado, USA

[6] T. Wagner, and J. Valasek, Digital Autoland Control Laws Using Quantitative Feedback Theory and Direct Digital Design,Journal of Guidance, Control, and Dynamics, Vol. 30, No. 5, 1399–1413, September-October, 2007.

[7] U.S. Military Specification MIL-F-8785C, November, 5, 1980.

[8] Anderson, J. D., Introduction to Flight, 5th Edison, Tata McGraw Hill Education Private Limited, New Delhi 2007

[9] Zipfel, P. H., Modeling and simulation of aerospace vehicle dynamics, AIAA, 2000

[10] Rauw, M., FDC 1.2-A Simulink Toolbox for Flight Dynamics and Control Analysis, Zeist, The Netherlands, 2001, 1, 7

[11] Tang, Y. L. and Kasturi, R., Runway detection in an image sequence, ISAT SPIE's Symposium on Electronic Imaging: Science and Technology, 1995, 181-190

[12] Woods, R. E., and Gonzalez, R. C. , Digital Image Processing, Prentice-Hall, Inc., 2nd Ed., New Jersey: 2002

[13] Marques, O., Practical Image and Video Processing using MATLAB, Wile, IEEE Press 2011

[14] Zuliani M., RANSAC toolbox for Matlab, Nov. 2008

[15] Saripalli S., Montgomery J. F. and Sukhatme G., Vision based Autonomous landing of unmanned aerial vehicle, May. 2002

[16] Tang, Y. L., Kasturi R., Runway detection in an image sequence, SPIE Vol. 2421 pp. 181-190